Frontiers of Physics
https://doi.org/10.1007/s11467-020-0960-x
Front. Phys.
15(4), 44301 (2020)

REVIEW ARTICLE

Experimental search for dark matter in China

Li Zhao[1,†], **Jianglai Liu**[1,2,‡]

[1] *School of Physics and Astronomy, Shanghai Jiao Tong University, Shanghai 200240, China*
[2] *Tsung-Dao Lee Institute, Shanghai Jiao Tong University, Shanghai 200240, China*
E-mail: [†] *zhaoli78@sjtu.edu.cn,* [‡] *jianglai.liu@sjtu.edu.cn*
Received March 18, 2020; accepted March 30, 2020

The nature of dark matter is one of the greatest mysteries in modern physics and astronomy. A wide variety of experiments have been carried out worldwide to search for the evidence of particle dark matter. Chinese physicists started experimental search for dark matter about ten years ago, and have produced results with high scientific impact. In this paper, we present an overview of the dark matter program in China, and discuss recent results and future directions.

Keywords dark matter, weakly interacting massive particle (WIMP), direct detection, indirect detection, Xenon, Germanium

Contents

1 Introduction 1
2 Direct detection experiments underground 2
2.1 PandaX dark matter experiment 3
2.2 CDEX dark matter program 5
3 Indirect detection in space: DAMPE satellite 8
4 Summary and perspectives 9
Acknowledgements 9
References 9

1 Introduction

The original concept of galactic invisible matter, the dark matter, has existed for almost a century, traditionally credited to Zwicky [1]. Convincing observations came around in 1970s from Rubin and Ford [2] on the rotation curves of many different galaxies, which strongly indicated the dominance of galactic dark matter over the normal stars and gases. To date, the gravitational effects of dark matter is evident from galaxies to galaxy clusters and superclusters (see, for example, Ref. [3]). During the past two decades, a standard model of the cosmology, the so-called ΛCDM model, has emerged [4]. This simple theoretical paradigm gives remarkable agreements to a diverse set of astrophysical data from the early universe (cosmic microwave background), large structure of the universe, galactic dynamics, etc. Precision cosmology studies using the data, e.g., by the Planck satellite [5], reveal that the universe is composed of 4.9% of baryonic matter, 26.8% of cold dark matter, and 68.3% of dark energy.

Microscopically, all known matters are made out of elementary particles, described elegantly by the Standard Model of particle physics [6]. The latest triumph of the theory is the discovery of the Higgs particle, the last missing particle in the theory, in 2012 [7, 8]. However, the Standard Model does not have any viable dark matter candidates. Many classes of theories on the physics beyond the Standard Model have been proposed in the past a few decades, for example, Supersymmetry [9], Extra Dimensions [10, 11], etc. These theories naturally predict heavy, neutral, and stable particles, which can be the particle dark matter candidates [12, 13]. Most of these theories also predict a feeble non-gravitational interactions among the dark matter particles and between the dark matter and normal matter. Generically, these dark matter particles are referred to as the Weakly Interacting Massive Particles (WIMPs), with a typical mass range between tens of GeV/c^2 to a few TeV/c^2.

The WIMP paradigm fits elegantly with the thermal history of the universe in the ΛCDM [4]. In the very early hot universe, WIMPs were in thermal equilibrium with ordinary matters, with a balance between the annihilation of WIMPs into ordinary particle-antiparticle pairs and backwards. Then as the universe expanded and cooled down, the annihilation reaction rates fell below the expansion, so WIMPs became a thermal relic. Coincidentally, most WIMP theories can reproduce the observed relic density of the dark matter – this so-called "WIMP Miracle" offers very compelling motivation for this class of models.

The feeble interactions between the WIMPs and normal matters also allow experimental studies in laboratories. There are three complementary approaches to identify WIMP dark matters. The first is the so-called direct detection, in which galactic WIMPs can interact with atomic nuclei in the target, resulting in nuclear recoils (NRs). Background gamma rays will result in electron recoils (ERs), which may be rejected experimentally. The second is the so-called indirect detections, to search for

*arXiv: 2004.04547.

© Higher Education Press and Springer-Verlag GmbH Germany, part of Springer Nature 2020

high energy particles produced by WIMP annihilations (e.g. from the center of the Galaxy). The third type is to produce "man-made" dark matter in high energy particle colliders. All three directions are pursued intensively worldwide. In China, experimental programs on dark matter direct and indirect detections have gained significant momentum in the past ten years. We shall present a review in these two areas in the rest of this paper.

2 Direct detection experiments underground

Due to the gravitational attractions, our Galaxy is surrounded by a large dark matter halo, extended far beyond the range of visible stars. The spacial distribution of the halo can be derived from the dynamics of our Galaxy. Close to the solar orbit, the nominal value for the dark matter mass density ρ_0 is 0.3 ± 0.1 GeV/cm^3 [14, 15]. The cold dark matter conjecture implies that these particles are ideal-gas-like with no preferred direction of motion except being gravitationally bound. Their velocity distribution is a Maxwell–Boltzmann distribution with a velocity cutoff at 650 km/s, corresponding to the galactic escape velocity [14, 15].

The direct detection of the dark matter utilizes the fact that the solar system orbits the Galactic center (and the dark matter halo on average) with a nearly circular velocity $v_0 = 220$ km/s [14, 15]. Therefore, relatively to the terrestrial detectors, the incoming dark matter particles carry an average momentum. The scattering of these dark matter particles with known matters in a standard target can be approximated as a non-relativistic two-body scattering. Direct detection experiments are designed to observe the low-energy (~10 keV) recoils of the nucleus struck rarely by an incoming WIMP. In principle, the electrons can also interact with the WIMPs, but the recoil energy is kinematically suppressed.

The recoil energy will be deposited in the target and converted into excitations such as photons, ionization electrons, or phonons, and can be detected by sensitive detectors. For example, one class of experiments operating at very low temperature (below 100 mK, also known as the micro-bolometer) is designed to detect the phonons. Representative experiments are CDMS (Si [16] and Ge [17]) and CRESST-II [18] ($CaWO_4$), which, at the same time, detect the ionization and photon signals, respectively. Another class of low noise semi-conductor experiments, for example CoGeNT [19] and CDEX [20], detects the ioniziation signals only. These experiments are sensitive to low mass WIMPs (10 GeV/c^2 and below), which produce relatively small recoil energy. On the other hand, noble liquid detectors such as XENON [21], LUX [22], PandaX [23] (xenon), DarkSide [24] and DEAP [25] (argon) typically detect scintillation photons, some in conjunction with ionization electrons. These experiments are powerful for the high mass WIMPs at the typical electroweak symmetry breaking scale (100 GeV/c^2 and above).

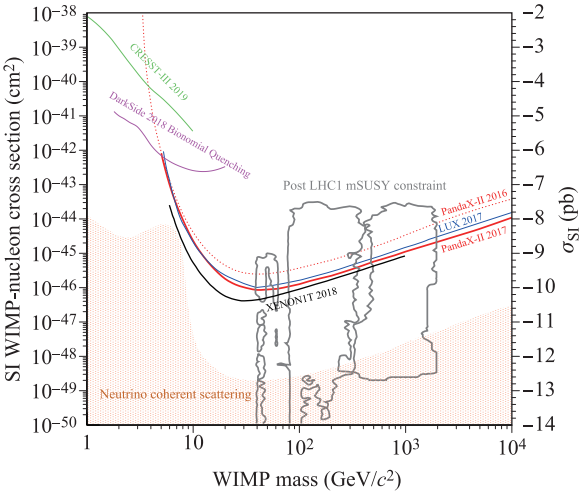


Fig. 1 The current 90% upper limits on WIMP-nucleon SI cross-section. See legend for the leading exclusion limits from PandaX-II [26, 27], XENON1T [28], DarkSide [29], and CRESST-III [30]. The dotted region at the lower left indicates the "limiting floor" to the sensitivity below which one could not identify dark matter from the coherent nuclear recoil background from the solar and atmospheric neutrinos.

For a given WIMP mass and the number of nuclear targets in a detector, the detected rate (limit) can be converted to a measurement (limit) of the scattering cross section between the WIMP and the nucleon. Recent world results are shown in Fig. 1. Despite very active search worldwide, none of the experiment has observed a convincing signal yet. Ultimately, the sensitivity of the direct detection experiments will be limited by the irreducible background due to coherent nuclear scattering of solar and atmospheric neutrinos - this is the so-called "neutrino floor" [31].

Due to the rarity of the dark matter signals, it is crucial to maintain an ultralow background environment. All dark matter direct detection experiments operate deep underground to reduce background events from the cosmic rays. The development of the undeground Laboratory provided a strong boost to the domestic dark matter experimental program. The initial development started in 2009, jointly by the Yalong River Hydropower Development Company and Tsinghua University, utilizing the 17.5 km horizontal access tunnels through the Jinping Mountain in Sichuan, China [32]. With a rock overburden of about 2400 meters, it is the deepest operating underground laboratory in the world. The muon flux is measured to be about 1/(m^2·week) [33], which minimizes the cosmogenically induced background. The horizontal tunnel facilitates the access.

The China Jinping underground Laboratory (CJPL) Phase-I (CJPL-I) lab consists of an experimental hall with an approximate dimension of 6 m (W)× 6 m (H)×40 m (L). The space is currently occupied by CDEX [20] and PandaX [23], the first generation dark matter direct detection experiments in China. A general

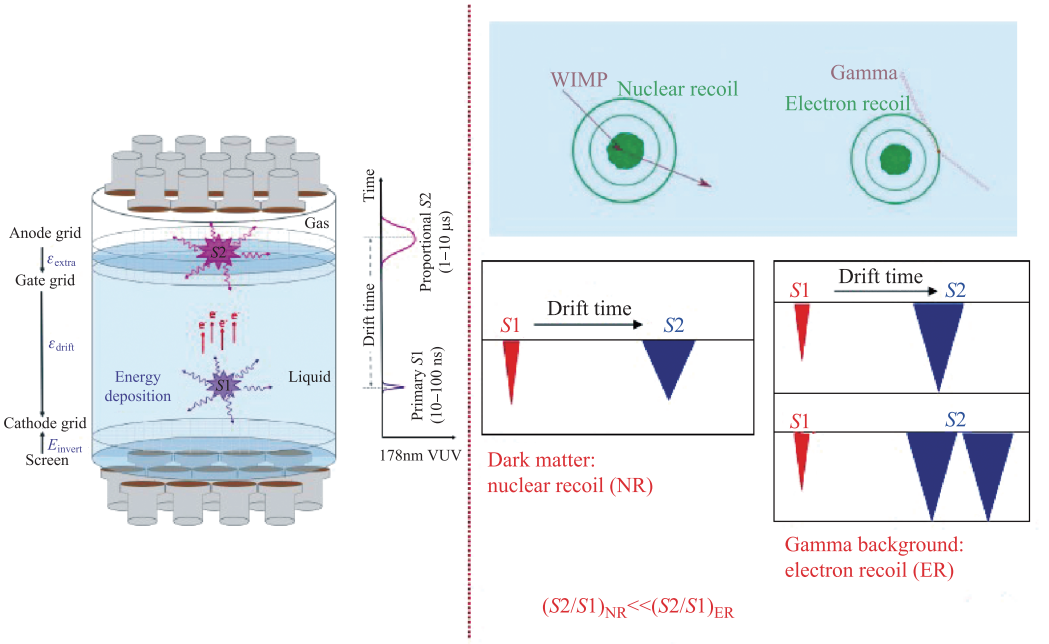


Fig. 2 The schematics of a two-phase xenon time projection chamber. Also shown are the illustrative signals for a gamma and WIMP event that cause either an electron or nuclear recoil.

purpose low radiopurity screening facility with a few high purity Germanium detectors is also operating in CJPL-I.

In 2015, much more experimental space has been excavated about 1500 m away from CJPL-I. This new space is now called CJPL-II, with eight experimental halls, each with dimensions of 14 m (W)×14 m (H)×65 m (L) [34]. China has committed a major development project to make CJPL-II a general purpose, deep underground, ultralow background national facility. Future projects in dark matter, neutrinos, nuclear astrophysics, geomechanics, etc., are being considered by the scientific committee of the laboratory.

2.1 PandaX dark matter experiment

The PandaX (Particle AND Astrophysical Xenon observatory) is a staged experimental program aiming to use xenon as the target to search for WIMP dark matter and to study the nature of neutrinos. The first (PandaX-I, 120 kg) and second stage (PandaX-II, 580 kg) experiments were completed in 2014 and 2019, respectively. Both experiments were located in CJPL-I. PandaX-I and PandaX-II utilized the so-called two-phase xenon time projection chamber (TPC) technique to detect the energy and position of the WIMP-nucleus scattering. The operation principle is shown in Fig. 2. A cryostat is filled with liquid xenon, with two closely-packed arrays of photomultiplier (PMTs) located at the top (gas) and bottom (liquid) of the chamber. The prompt scintillation photons collected by the PMTs is referred as the $S1$ signal. To collect the ionization electrons, a drift electric field is applied between a light transmitting cathode and gate electrodes, located at bottom and top of the liquid xenon, respectively. A much stronger electrical field is set between the gate (in liquid) and anode (in gas). This so-called extraction field extracts the ionized electrons into the gaseous xenon, in which region secondary electroluminescence photons are subsequently produced close to the top PMT array. This delayed flash of photons is referred to as the $S2$ signal. A three-dimensional imaging of the interaction vertex can be achieved by using the pattern of $S2$ collected by the top PMT array (horizontal position) and the time separation between the $S1$ and $S2$ (vertical position). Peripheral background coming from outside of the detector can be significantly suppressed by fiducialization. Events with multiple $S2$s (Fig. 2) from multiscattering of the background gammas or neutrons are also rejected. For the remaining single-scatter events, due to the difference in the ionization capability of the recoiling electron (stronger) and nucleus (weaker), the fraction of energy carried by ionized electrons is different between the two. Therefore the ratio $S2/S1$ is another powerful discriminant against the ER background.

The superior potential of the liquid xenon TPC had been demonstrated by several experiments, including XENON10 [35], XENON100 [21], ZEPLIN [36], and LUX [22].

At CJPL-I, a passive shielding to suppress ambient neutrons and gamma rays was constructed and used in both PandaX-I and PandaX-II. From outside to inside, it consisted of 40 cm of Polyethylene (PE), 20 cm of lead, 20 cm of PE, and 5 cm oxygen-free high thermal conductivity copper (OFHC). The innermost shield is a vacuum copper vessel, which is also a vacuum jacket for the cryostat

and an ambient radon barrier.

The PandaX-I TPC was specially designed for a high light yield thus low energy threshold, to search for low-mass WIMPs. The TPC field cage was enclosed by a cylindrical polytetrafluoroethylene (PTFE) wall with 15 cm in height and 60 cm in diameter. The pancake-shaped target was to reduce photon loss before it reached the PMTs. For the PMTs arrays, there were 143 Hamamatsu R8520-406 1-inch square PMTs at the top and 37 Hamamatsu R11410-MOD 3-inch PMTs at the bottom. After series of engineering runs, the dark matter search data were collected between March and October of 2014 [37, 38]. The total exposure was 54×80.1 kg-day. A blind analysis was carried out. Seven events in the signal region were found with 6.9 ± 0.6 expected background events, consistent with no excess over background. The exclusion limit to the spin-independent (SI) isoscalar WIMP-nucleon scattering cross section is shown in Fig. 3. At the 90% confidence level, the limit for WIMP mass below 5.5 GeV/c^2 was the tightest reported constraints among all liquid xenon experiments by that time. The exclusion limit strongly disfavored the claimed signal regions by DAMA-LIBRA [39], CoGeNT [40], CRESST-II [18], and CDMS-Si [16]. This result was a major milestone in the development of the PandaX program.

To improve the sensitivity to WIMPs, an immediate upgrade towards PandaX-II was carried out in 2015. The key difference in PandaX-II was an enlarged TPC to accommodate a 580 kg liquid xenon target. The TPC was 60 cm high with a diameter of 60 cm. A total of 110 Hamamatsu 3-inch R11410-20 PMTs with improved quantum efficiency were implemented. To suppress background, a new cryostat was made by radiopure stainless steel [41]. In the region between the TPC field cage and the inner cryostat, two rings of 24 Hamamatsu 1-inch R8520-406 PMTs were installed at the top and bottom to further veto external background events.

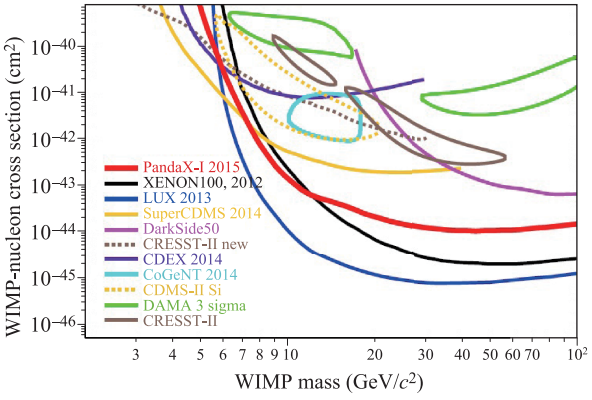


Fig. 3 The 90% confidence level upper limit for SI isoscalar WIMP-nucleon cross section for the PandaX-I experiment (red curve). Results from other experiments are overlaid for comparison (see legend, contours are claimed signal regions, lines are exclusion limits). Reproduced from Ref. [38].

Initial dark matter data in PandaX-II were collected from November to December in 2015 (Run 8). The run was stopped after the identification of a high ^{85}Kr background (a β-emitter with an abundance of about 2×10^{-11} in natural krypton), likely introduced by an air leak. The krypton-to-xenon atomic ratio inferred from the data was about 400 part-per-trillion or ppt. The data taking was resumed in March 2016 after a krypton distillation campaign, which reduced the krypton level by about a factor of 10, leading to a record low background rate of 2×10^{-3} evt/(day·kg·keV) by that time. A low background data set was collected between March and June 2016 (Run 9), which, in combination with Run 8, provided a leading WIMP exposure of 33 ton-day. In the NR signal region, only one event was identified with a mean expected background of 2.5 events. A stringent upper limit was set on the elastic SI WIMP-nucleon scattering cross section, with the lowest excluded cross section of 2.5×10^{-46} cm^2 for a WIMP mass of 40 GeV/c^2 [26], which improved from the previous best limit from LUX [42] by a factor of 2.5. In addition, since the net spin of the xenon nucleus is mostly carried the odd-neutron isotopes, ^{129}Xe and ^{131}Xe, the same data provided a leading limit on the spin-dependent (SD) WIMP-neutron interaction [43].

After Run 9, to make an accurate calibration of the detector response to ER events, a tritiated methane injection was carried out, a technique pioneered by the LUX collaboration [44]. After the calibration, to remove the residual tritium left in the detector and to further suppress krypton background, a second distillation campaign was carried out in CJPL-II. The tritium was largely removed and the krypton level was reduced to about 6 ppt. Another low background data set (Run 10) was collected from March to July 2017. The ER background level of was 0.8×10^{-3} evt/(day·kg·keV), 2.5 times suppressed from that in Run 9, yet no excess was found in the signal region. The new limit to spin-independent WIMP-nucleon interaction (Fig. 4) was released in Ref. [27] by combining Run 9 and Run 10, with a dark matter exposure of 54 ton-day. This represented the most stringent limit for a WIMP mass greater than 100 GeV/c^2 by that time.

The data from PandaX-II were also used to study non-WIMP dark matter particles and interactions. For example, axion is a pseudoscalar particle dark matter candidate, originally proposed to mandate the observed charge-parity or CP symmetry in the strong interactions [47, 48]. Assuming that axions can couple to electrons, solar axion or galactic axion-like particles (ALPs) were searched using the PandaX-II data in the ER region [49]. Due to the low ER background rate and large exposure, stringent limits on the dimensionless axion-electron coupling constant g_{Ae} for both scenarios were set, shown in Fig. 5. The PandaX-II data were also used, the first time, to search for a special dark matter-nucleon interactions in which the interaction portal is a light mediator particle with a finite kinematic mixing to the known standard model gauge particles, e.g.

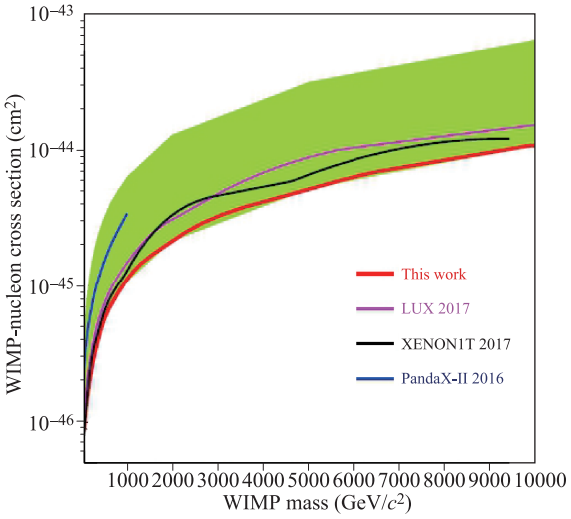


Fig. 4 The 90% C. L. upper limits for the SI WIMP-nucleon cross section from the combination of the data from PandaX-II Run 9 and Run 10 (red solid). The 1-σ sensitivity band is shown in green respectively. Data from XENON1T 2017 [45] and LUX 2017 [46] are overlaid for comparison. Reproduced from Ref. [27].

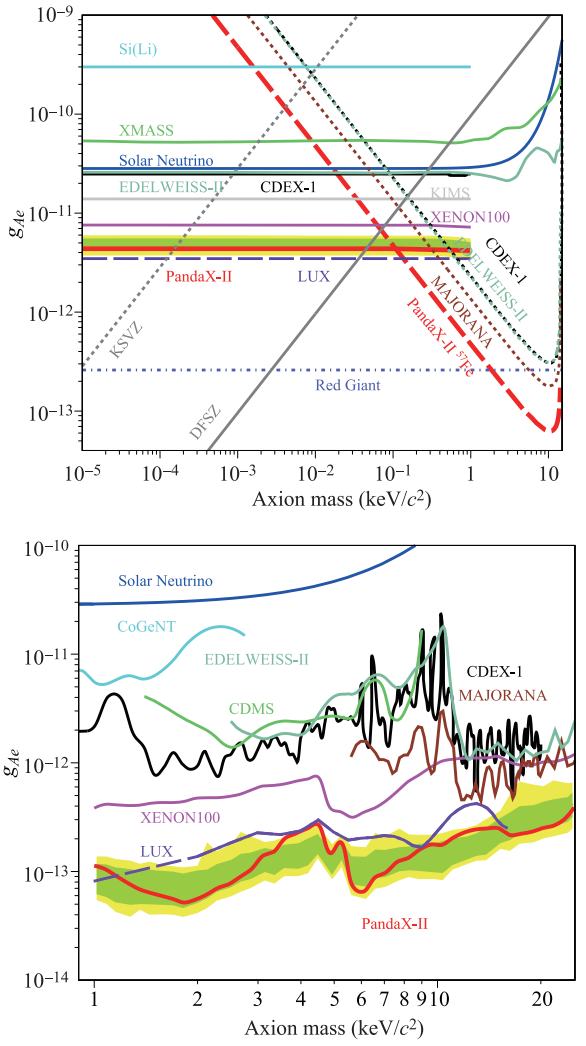


Fig. 5 Axion-electron coupling constant g_{Ae} vs. the axion mass, from PandaX-II Run 9 data, for solar axion (top) and galactic axion-like particles (bottom). Reproduced from Ref. [49].

a photon [50]. The self-interaction between dark matters carried by such light mediator is of particular interest to solve the so-called "diversity problem" in the galactic rotational curves [51]. For other more complex interactions between the WIMP and nucleon beyond the standard SI and SD interactions, a more general analysis under the effective field theory framework is presented in Ref. [52], in which the state-of-art nuclear matrix element calculations for xenon nuclei is applied. Leading constraints were set on many different forms of interactions.

The PandaX-II operation was completed in July 2019, with an approximate total accumulated exposure of 140 ton-day for dark matter search. The WIMP analysis on the full data set is ongoing. Series of detector systematics studies and technological development were also carried out. Since natural xenon contains 8.9% of ^{136}Xe, a double β-decay isotope (simultaneous conversion of two neutrons into two protons and electrons in the nucleus), the PandaX-II collaboration also published a new result on the neutrinoless double-beta decay (NLDBD) search of ^{136}Xe (with a decay Q value of 2.458 MeV) using the data [53]. Such a decay, if found in nature, is a direct proof that neutrino is its own anti-particle (so-called Majorana particle), which would also have profound consequence in particle physics and cosmology. With the PandaX-II data, a lower limit for the decay half-life of 2.1×10^{23} years was set at 90% confidence level, corresponding to an upper limit of the effective Majorana neutrino mass between 1.4 to 3.7 eV/c^2. This is the first NLDBD result from a liquid xenon dark matter experiment, which also demonstrates the feasibility to carry out more sensitive searches in future experiments.

The new generation of the PandaX dark matter experiment is a liquid xenon TPC with a sensitive target of 4-ton in mass, the PandaX-4T. The expected lowest sensitivity to WIMP-nucleon spin-independent cross section is 6×10^{-48} cm^2 at 40 GeV/c^2 with a 6-ton-year exposure [54]. PandaX-4T is located in the B2 hall of the CJPL-II. From the fall of 2019, the subsystem components of PandaX-4T detector were transported gradually to CJPL-II. The assembly of the detector is expected to take a full year, then the experiment will switch to its commissioning phase. The future generation of the PandaX experiment is also being planned as a multi-purpose dark matter and neutrino observatory, with an ultimate WIMP sensitivity to the "neutrino floor" [55].

2.2 CDEX dark matter program

In 2009, the China Dark matter EXperiment (CDEX) collaboration was established. The main goal of CDEX is to pursue studies on low mass WIMPs (<10 GeV/c^2). To

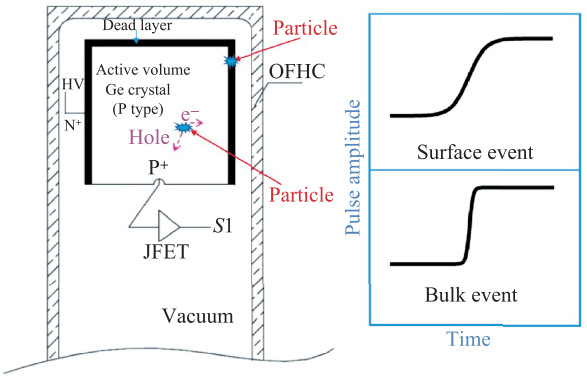


Fig. 6 Diagram of the PPCGe detector and sketches of the waveform for the surface and bulk events. Reproduced from Ref. [56].

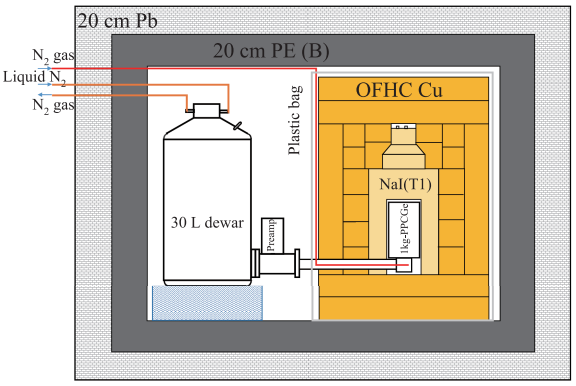


Fig. 7 Schematic diagram of the design of CDEX-1. The PPCGe detector was enclosed by an active shielding with NaI(Tl) crystal scintillator and a passive shielding. Reproduced from Ref. [61].

achieve this, it is necessary to develop a dark matter detector with a ultra-low energy threshold. The CDEX experiment employs the so-called P-type point-contact high purity Germanium as the detector. Its modular structure and simple cryogenic system make it relatively easy to scale up to large detector arrays.

The point-contact technology was developed several decades ago based on the more generally-used coaxial Germanium detector. In order to achieve an ultra-low energy threshold, the area of the electrode is made to be only of a mm-scale, so its capacitance can achieve the level of few pF. This technology provides the possibility to decrease the energy threshold down to a level of a couple of hundreds eV. Collaborating with the Canberra Company, the CDEX collaboration developed a P-type point-contact Germanium (PPCGe) detector with a mass of 1 kg (CDEX-1). The structure of CDEX-1 is shown in Fig. 6. The crystal cylinder has a n^+ type contact on the outer surface and a tiny p^+ type contact as the central electrode. The electron-hole pairs are produced as particles interact with Ge atoms. Under electrical field, electrons and holes drift to the opposite electrodes. During the drift, signals will be induced in the p^+ and n^+ electrodes. Due to the structure of the electrode, holes close to the surface drift much slower, therefore the signal pulse has a long rise time and a relatively small amplitude. Therefore, such detector has the ability to differentiate surface (background-like) and bulk (signal-like) events.

To shield the gamma rays or neutron backgrounds from the ambient environment, a passive shielding structure has been setup for CDEX. The outer shielding is a 1 m thick PE "house", containing the entire CDEX setup. The structure of the inner shielding is shown in Fig. 7, including a 20 cm of lead layer to stop gamma rays and a 20 cm layer of boron-loaded PE for neutron absorption, from outside to inside. A 20 cm thick OFHC surrounds the cryostat of the PPCGe detector to further decrease the residual gamma background. At the same time, the volume is purged by dry nitrogen to suppress radon contamination. In order to further reduce the background, an active anti-coincidence NaI(Tl) detector enclosing the PPCGe was later implemented during the operation.

In the initial data taking period of CDEX (CDEX-1A), in order to study the background, the bulk surface cut was not applied, nor was the anti-coincidence detector installed. In total, 14.6 kg-days of data were collected in 2012. This led to the first scientific result of CDEX-1A [57], in which 400 $\mathrm{eV_{ee}}$ (electron-equivalent energy) was chosen as the analysis energy threshold. The upper limits on WIMP SI cross section at different WIMP masses were close to the bounds from the TEXONO [58] experiment, using the same PPCGe detector approach. The second operation period started in 2014, with the anti-coincidence detector implemented. CDEX-1A collected a complete exposure of 335.6 kg-day, with a rate and spectrum above the 475 $\mathrm{eV_{ee}}$ threshold consistent with the background model. New constraints on the SI and SD WIMP-nucleon interactions were set in Refs. [59, 61], which excluded the claimed signal region from CoGeNT using identical PPCGe technology [40]. The claimed signal region from the excess of the DAMA-LIBRA experiment [39] was also strongly disfavored.

To further improve the energy threshold, a new 1-kg PPCGe (CDEX-1B) was deployed in 2014. An analysis threshold of 160 $\mathrm{eV_{ee}}$ [60] was achieved, a significant step forward from CDEX-1A. With a total stable data taking span of 4.2 years, CDEX-1B was able to make an analysis on the annual modulation of the detected event rate. Due to Earth's motion in solar orbit, an annual modulation in the Earth's velocity relative to the galactic DM halo thereby the collision rate with target nucleus is expected for galactic dark matters. Both DAMA-LIBRA and the CoGeNT experiments have claimed such an evidence in their data [39, 62]. The WIMP-nucleon SI interaction derived from the CDEX-1B annual modulation analysis excluded the claims from DAMA-LIBRA and CoGeNT by 99.99% and 98.0% confidence level [63] (Fig. 8).

For dark matter with lower masses (less than 1 GeV/c^2), the elastic collision energy with atomic nucleus would be

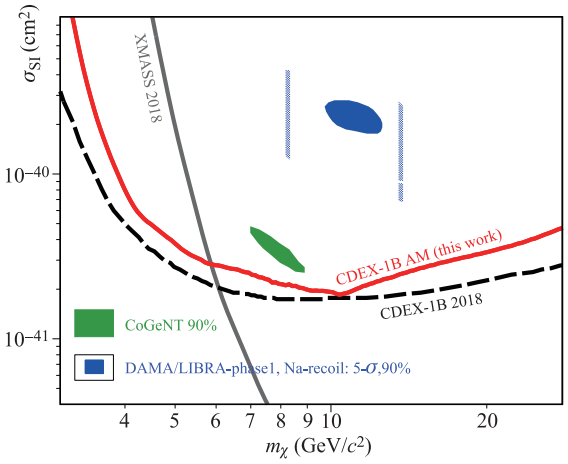


Fig. 8 Limits at 90% C.L. from CDEX-1B annual modulation analysis (red) on spin-independent WIMP-nucleon cross section. Also shown are other annual modulation-based results: upper limits of XMASS-1 (dark gray) [64], and the allowed regions from DAMA/LIBRA phase1 [39] and CoGeNT [62]. Constraints from the CDEX-1B time-integrated spectral analysis [60] are also displayed (black dotted line) as comparison. Reproduced from Ref. [63].

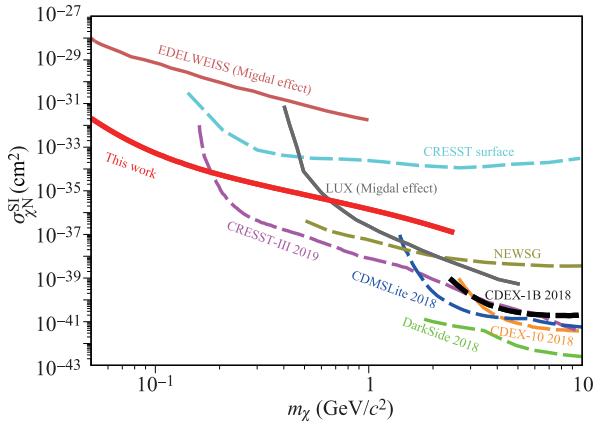


Fig. 9 Upper limits at 90% C.L. on the SI dark matter-nucleon cross section derived by binned Poisson analysis using the CDEX-1B experiment data, with several benchmark experiments [29, 66–68] superimposed. Limits from nuclear recoil-only analysis with the same data set is shown as well (black dash line). The limit with the Migdal effect incorporated (red solid line) provides the best sensitivities for a dark matter mass between 50 and 180 MeV/c^2. Reproduced from Ref. [69].

too small to be detected by traditional technology. An interesting subdominant atomic effect, the so-called Migdal effect [65], was recently brought up to great attention. In short, the displacement between the struck nucleus and the surrounding electrons could sometimes produce additional detectable excitation energy above the detector threshold, which in effect widens the dark matter mass range toward the lower end. The CDEX collaboration performed this analysis (Fig. 9), which lowered the mass range by more than one order of magnitude (to about 50 MeV/c^2) in comparison to the traditional analysis [69].

In addition to the improvement in energy threshold, the CDEX collaboration also made significant progress in scaling up the detector. The upgraded CDEX experiment with a total detector mass of about 10 kg, CDEX-10, was under operation since 2017. Three triple-unit PPCGe strings (C10A,B,C) were directly immersed in liquid nitrogen (see Fig. 10). The first physics dataset (102.8 kg-days) from one detector (C10B-Ge1) was obtained with an analysis threshold of 160 eV$_{ee}$. This results into a leading constraint on SI WIMP-nucleon cross section at 8×10^{-42} cm^2 for a WIMP mass of 5 GeV/c^2 [67].

The data from CDEX was also used to search for other rare process. For example, CDEX-1A and CDEX-1B data provided constraints on axion-electron g_{Ae} for ALPs and vector bosonic dark matter at keV-scale and below [70, 71]. Since the natural Germanium contains 7.8% of ^{76}Ge, another double β-decay isotope, the full CDEX-1A data set was analyzed to set a lower limit on the half-life of NLDBD of ^{76}Ge to be 6.4×10^{22} years [72], translating into an upper limit on the effective Majorana neutrino mass of about 5.0 eV/c^2. Lately the results of dark photon searches were reported based on the CDEX-10 data, probing new parameter space with masses from 10 to 300 eV/c^2 in direct detection experiments [73].

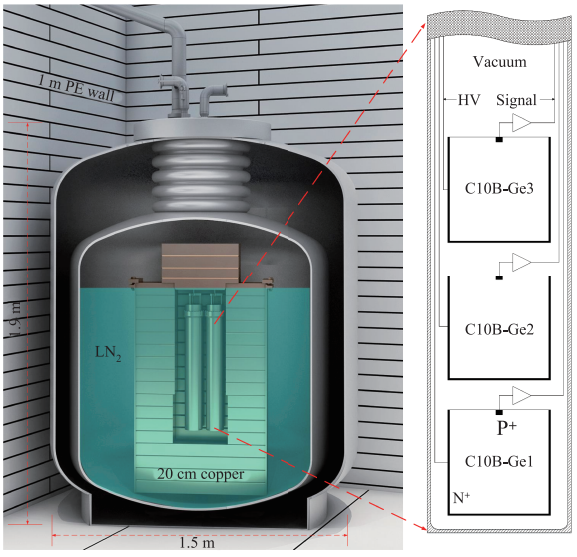


Fig. 10 Configuration of CDEX-10 experimental setup (left) and C10B detector layout in the string (right). Each detector string has three PPCGe detectors. Reproduced from Ref. [67].

The long-term goal of CDEX program is a ton-scale Germanium experiment (CDEX-1T) searching for dark matter and NLDBD. In the C1 hall of CJPL-II, a pit with a diameter of 18 m and a depth of 18 m was constructed to house the future experiment. Gearing toward the future, CDEX researchers are developing critical technologies such as detector-grade Germanium crystal growth and ultralow background techniques.

3 Indirect detection in space: DAMPE satellite

As mentioned in the introduction, two WIMP particles, when encounter, have a finite probability to annihilate and produce the standard model particles. Therefore, one can look for the signature of dark matter by observing energetic γ rays, neutrinos or charged cosmic ray particles as the annihilation or decay products. However, these high energy particles could also be produced by standard astrophysical processes. Since dark matter particle has a specific mass, the direct annihilation products should have a narrow line feature. The decay products or secondary particles from the annihilation would be distributed in a particular energy range. The dark matter indirect detection is to look for excess and features in the energy spectrum of the detected particles, on top of the expected background spectrum from known astrophysical processes.

The satellite-borne particle/astroparticle physics experiments started several decades ago. The cosmic electrons, positrons, and gamma rays have been measured by a number of satellite-borne experiments, for example, PAMELA [74], FERMI [75], AMS-02 [76], CALET [77], and ISS-CREAM [78]. These experiments covered an energy range up to 3 TeV. An intriguing broad excess in the positron to electron ratio above a few tens GeV was found by PAMELA [79]. This triggers broad interests in the community to understand both the dark matter signals as well as that from the local astrophysical background.

The DArk Matter Particle Explorer (DAMPE) collaboration, led by the Purple Mountain Observatory of the Chinese Academy of Sciences (CAS), includes nine participating institutes from China, Switzerland and Italy. DAMPE is one of the five satellite missions funded by the Strategic Pioneer Research Program in Space Science of the CAS. The main scientific objective of DAMPE is to measure electrons and gammas with much higher energy resolution and energy range than previous experiments to identify possible Dark Matter signatures.

A schematics of the DAMPE detector is shown in Fig. 11. It consists of a Plastic Scintillator strip Detector (PSD), a Silicon-Tungsten tracKer-converter (STK), a BGO imaging calorimeter and a NeUtron Detector (NUD). The PSD measures the charge of incident particles and provides charged-particle background rejection for gamma rays (anti-coincidence detector). The STK measures the charges and the trajectories of charged particles. The BGO calorimeter, with a total depth of about 32 radiation lengths, allows the measurement of the energy of incident particles with high resolution and to provide efficient electron/hadron identification. Finally, the NUD provides an independent measurement to further improve the electron/hadron identification. With the combination of these four sub-detectors, DAMPE has achieved a very effective rejection of the hadronic cosmic-ray background, and a much improved energy resolution for cosmic ray measurements.

In between 2014 and 2015, the DAMPE engineering qualification model was tested using test beams at CERN. These tests demonstrated excellent energy resolution for electrons and gamma ray (less than 1.2% for energy > 100 GeV), and verified its powerful electron/proton discrimination capabilities.

DAMPE was launched on Dec. 17, 2015 into a sun-synchronous orbit at the altitude of 500 km. The e^+e^- analysis result from the data between 27 December 2015 and 8 June 2017 was published in 2017. The total cosmic ray e^+e^- spectrum measured by DAMPE is shown in Fig. 12. In the energy range from hundreds GeV to a few TeV, these data have unprecedented high energy resolution and low background. Interestingly, the data can be fitted with a broken power-law (with a break at 0.9 GeV) rather than a single power law. In addition, a new feature was found at around 1.4 TeV, which has triggered many theoretical discussions on the possible dark matter origin (see, for example, Refs. [82–87]). DAMPE is continuing

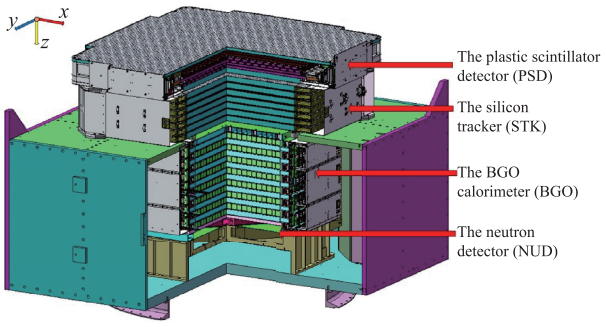


Fig. 11 Schematic view of the DAMPE detector. Reproduced from Ref. [80].

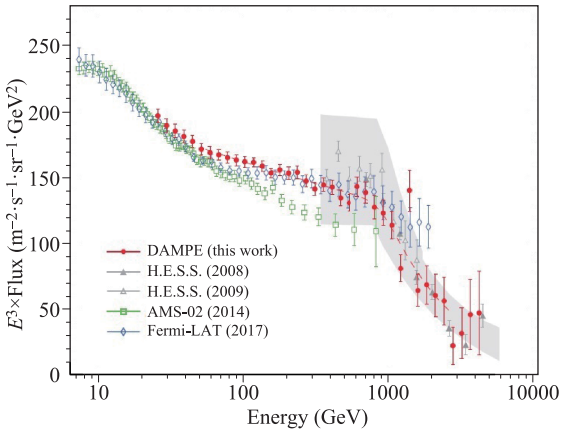


Fig. 12 The summed cosmic ray electrons and positrons spectrum ($\times E^3$) measured by DAMPE. The red dashed line represents a smoothly broken power-law model that best fits the DAMPE data in the range from 55 GeV to 2.63 TeV. Some results from HESS, AMS-02, and Fermi-LAT are overlaid for comparison (see legend). Reproduced from Ref. [81].

with data taking, and the data with more statistics are expected in the near future. Future upgrade is also under consideration by the collaboration.

4 Summary and perspectives

After almost a century since it was initially proposed, the nature of dark matter remains mysterious. In the past decade, there is an increasing involvement from the Chinese community in the experimental pursue of the dark matter, with great incentive from the development of the Jinping underground laboratory and the Chinese scientic satellite programs. In this paper, we present the progress of the China-led experiments in the direct and indirect dark matter searches. The sensitivity of these highly complementary efforts reach the forefront of the global dark matter hunt, demonstrating also the technical capability and scientific expertise of the Chinese community. Ambitious upgrades are also being planned for the future, which may open up the window for a major scientific discovery.

Acknowledgements The authors thank Prof. Qian Yue and Dr. Litao Yang from Tsinghua University, and also appreciate Prof. Jin Chang from Purple Mountain Observatory for their generous help with the content of this paper. This work was supported in part by the Double First Class plan of the Shanghai Jiao Tong University, the Key Laboratory for Particle Physics and Cosmology, Ministry of Education, and the Chinese Academy of Sciences Center for Excellence in Particle Physics. We also thank supports from the National Natural Science Foundation of China, Ministry of Science and Technology, Office of Science and Technology, Shanghai Municipal Government, and the Hongkong Hongwen Foundation and Tencent Foundation in China.

References

1. F. Zwicky, On the masses of nebulae and of clusters of nebulae, *Astrophys. J.* 86, 217 (1937)
2. V. C. Rubin and W. K. J. Ford, Rotation of the Andromeda nebula from a spectroscopic survey of emission regions, *Astrophys. J.* 159, 379 (1970)
3. S. W. Allen, A. E. Evrard, and A. B. Mantz, Cosmological parameters from observations of galaxy clusters, *Annu. Rev. Astron. Astrophys.* 49(1), 409 (2011)
4. E. W. Kolb and M. S. Turner, The Early Universe, Addison-Wesley Publishing Company, 1990
5. P. A. R. Ade, et al. (Planck Collaboration), Planck 2013 results. XVI. Cosmological parameters, *Astron. Astrophys.* 57, A16 (2013)
6. R. Oerter, The Theory of Almost Everything: The Standard Model, the Unsung Triumph of Modern Physics, Penguin Group, 2006
7. G. Aad, et al. (ATLAS Collaboration), Observation of a new particle in the search for the standard model Higgs boson with the ATLAS detector at the LHC, *Phys. Lett. B* 716, 1 (2012)
8. S. Chatrchyan, et al. (CMS Collaboration), Observation of a new boson at a mass of 125 GeV with the CMS experiment at the LHC, *Phys. Lett. B* 716(1), 30 (2012)
9. G. Kane and M. Shifman (Eds.), The Supersymmetric World — The Beginnings of the Theory, World Scientific, Singapore, 2000
10. N. Arkani-Hamed, S. Dimopoulos, and G. Dvali, The hierarchy problem and new dimensions at a millimeter, *Phys. Lett. B* 429(3–4), 263 (1998)
11. L. Randall and R. Sundrum, Large mass hierarchy from a small extra dimension, *Phys. Rev. Lett.* 83(17), 3370 (1999)
12. G. Jungman, M. Kamionkowski, K. Griest, and S. D. Matters, Supersymmetric dark matter, *Phys. Rep.* 267(5–6), 195 (1996)
13. G. Servant and T. M. P. Tait, Is the lightest Kaluza–Klein particle a viable dark matter candidate? *Nucl. Phys. B* 650(1–2), 391 (2003)
14. M. C. Smith, G. R. Ruchti, A. Helmi, R. F. G. Wyse, J. P. Fulbright, K. C. Freeman, J. F. Navarro, G. M. Seabroke, M. Steinmetz, M. Williams, O. Bienayme, J. Binney, J. Bland-Hawthorn, W. Dehnen, B. K. Gibson, G. Gilmore, E. K. Grebel, U. Munari, Q. A. Parker, R. D. Scholz, A. Siebert, F. G. Watson, and T. Zwitter, The RAVE survey: Constraining the local galactic escape speed, *Mon. Not. R. Astron. Soc.* 379(2), 755 (2007)
15. C. Savage, K. Freese, and P. Gondolo, Annual modulation of dark matter in the presence of streams, *Phys. Rev. D* 74(4), 043531 (2006)
16. R. Agnese, et al. (CDMS Collaboration), Silicon detector dark matter results from the final exposure of CDMS II, *Phys. Rev. Lett.* 111(25), 251301 (2013)
17. Z. Ahmed, et al. (CDMS Collaboration), Results from a low-energy analysis of the CDMS II Germanium data, *Phys. Rev. Lett.* 106(13), 131302 (2011)
18. G. Angloher, et al. (CRESST Collaboration), Results on low mass WIMPs using an upgraded CRESST-II detector, *Eur. Phys. J. C* 774(12), 3184 (2014)
19. C. E. Aalseth, et al. (CoGeNT Collaboration), CoGeNT: A search for low-mass dark matter using p-type point contact Germanium Detectors, *Phys. Rev. D* 88(1), 012002 (2013)
20. K. J. Kang, et al. (CDEX Collaboration), Introduction to the CDEX experiment, *Front. Phys.* 8(4), 412 (2013)
21. E. Aprile, et al. (XENON100 Collaboration), Dark matter results from 225 live days of XENON100 data, *Phys. Rev. Lett.* 109(18), 181301 (2012)
22. D. S. Akerib, et al. (LUX Collaboration), First results from the LUX dark matter experiment at the Sanford underground research facility, *Phys. Rev. Lett.* 112(9), 091303 (2014)
23. X. G. Cao, et al. (PandaX Collaboration), PandaX: A liquid xenon dark matter experiment at CJPL, *Sci. China Phys. Mech. Astron.* 57(8), 1476 (2014)

24. T. Alexander, et al. (DarkSide Collaboration), DarkSide search for dark matter, *J. Instrum.* 8(11), C11021 (2014)
25. M. Boulay, B. Cai, and the Deap/Clean Collaboration, Dark matter search at SNOLAB with DEAP-1 and DEAP/CLEAN-3600, *J. Phys. Conf. Ser.* 136(4), 042081 (2008)
26. A. Tan, et al. (PandaX Collaboration), Dark matter results from first 98.7 days of data from the PandaX-II experiment, *Phys. Rev. Lett.* 117(12), 121303 (2016)
27. X. Cui, et al. (PandaX Collaboration), Dark matter results from 54-ton-day exposure of PandaX-II experiment, *Phys. Rev. Lett.* 119(18), 181302 (2017)
28. E. Aprile, et al. (XENON Collaboration), Dark matter search results from a one ton-year exposure of XENON1T, *Phys. Rev. Lett.* 121(11), 111302 (2018)
29. P. Agnes, et al. (DarkSide Collaboration), Low-mass dark matter search with the DarkSide-50 experiment, *Phys. Rev. Lett.* 121(8), 081307 (2018)
30. A. H. Abdelhameed, et al. (CRESST collaboration), First results from the CRESST-III low-mass dark matter program, *Phys. Rev. D* 100(10), 102002 (2019)
31. J. Billard, L. Strigari, and E. Figueroa-Feliciano, Implication of neutrino backgrounds on the reach of next generation dark matter direct detection experiments, *Phys. Rev. D* 89(2), 023524 (2014)
32. K. J. Kang, J. P. Cheng, Y. H. Chen, Y. J. Li, M. B. Shen, S. Y. Wu, and Q. Yue, Status and prospects of a deep underground laboratory in China, *J. Phys. Conf. Ser.* 203, 012028 (2010)
33. Y. C. Wu, X. Q. Hao, Q. Yue, Y. J. Li, J. P. Cheng, K. J. Kang, Y. H. Chen, J. Li, J. M. Li, Y. L. Li, S. K. Liu, H. Ma, J. B. Ren, M. B. Shen, J. M. Wang, S. Y. Wu, T. Xue, N. Yi, X. H. Zeng, Z. Zeng, and Z. H. Zhu, Measurement of cosmic ray flux in the China JinPing underground laboratory, *Chin. Phys. C* 37(8), 086001 (2013)
34. J. P. Cheng, K. J. Kang, J. M. Li, J. Li, Y. J. Li, Q. Yue, Z. Zeng, Y. H. Chen, S. Y. Wu, X. D. Ji, and H. T. Wong, The China Jinping underground laboratory and its early science, *Annu. Rev. Nucl. Part. Sci.* 67(1), 231 (2017)
35. J. Angle, et al. (XENON Collaboration), First results from the XENON10 dark matter experiment at the Gran Sasso National Laboratory, *Phys. Rev. Lett.* 100(2), 021303 (2008)
36. G. J. Alner, et al. (ZEPLIN-II Collaboration), Limits on spin-dependent WIMP-nucleon cross-section from the ZEPLIN-II data, *Phys. Lett. B* 653, 161 (2007)
37. M. J. Xiao, et al. (PandaX Collaboration), First dark matter search results from the PandaX-I experiment, *Sci. China Phys. Mech. Astron.* 57(11), 2024 (2014)
38. X. Xiao, et al. (PandaX Collaboration), Low-mass dark matter search results from full exposure of the PandaX-I experiment, *Phys. Rev. D* 92(5), 052004 (2015)
39. R. Bernabei, et al. (DAMA Collaboration), Final model independent result of DAMA/LIBRA-phase1, *Eur. Phys. J. C* 73(12), 2648 (2013)
40. C. E. Aalseth, et al. (CoGeNT Collaboration), Maximum likelihood signal extraction method applied to 3.4 years of CoGeNT data, arXiv:1401.6234v3 (2014)
41. T. Zhang, C. Fu, X. Ji, J. Liu, X. Liu, X. Wang, C. Yao, and X. Yuan, Low background stainless steel for the pressure vessel in the PandaX-II dark matter experiment, *J. Instrum.* 11(09), T09004 (2016)
42. D. S. Akerib, et al. (LUX Collaboration), Improved limits on scattering of weakly interacting massive particles from reanalysis of 2013 LUX data, *Phys. Rev. Lett.* 116(16), 161301 (2015)
43. C. Fu, et al. (PandaX Collaboration), Spin-dependent WIMP-nucleon cross section limits from first data of PandaX-II experiment, *Phys. Rev. Lett.* 118, 071301 (2017)
44. D. S. Akerib, et al. (LUX Collaboration), Tritium calibration of the LUX dark matter experiment, *Phys. Rev. D* 93(7), 072009 (2016)
45. E. Aprile, et al. (XENON Collaboration), First dark matter search results from the XENON1T experiment, *Phys. Rev. Lett.* 119(18), 181301 (2017)
46. D. S. Akerib, et al. (LUX Collaboration), Results from a search for dark matter in the complete LUX exposure, *Phys. Rev. Lett.* 118(2), 021303 (2017)
47. S. Weinberg, A new light boson? *Phys. Rev. Lett.* 40(4), 223 (1978)
48. F. Wilczek, Problem of strong P and T invariance in the presence of instantons, *Phys. Rev. Lett.* 40(5), 279 (1978)
49. C. Fu, et al. (PandaX Collaboration), Limits on axion couplings from the first 80 days of data of the PandaX-II experiment, *Phys. Rev. Lett.* 119(18), 181806 (2017)
50. X. Ren, et al. (PandaX Collaboration), Constraining dark matter models with a light mediator at the PandaX-II experiment, *Phys. Rev. Lett.* 121(2), 021304 (2018)
51. A. Kamada, M. Kaplinghat, A. B. Pace, and H. B. Yu, Self-interacting dark matter can explain diverse galactic rotation curves, *Phys. Rev. Lett.* 119(11), 111102 (2017)
52. J. Xia, et al. (PandaX Collaboration), PandaX-II constraints on spin-dependent WIMP-nucleon effective interactions, *Phys. Lett. B* 792, 193 (2019)
53. K. Ni, et al. (PandaX Collaboration), Searching for neutrino-less double beta decay of Xe-136 with PandaX-II liquid xenon detector, *Chin. Phys. C* 43, 113001 (2019)
54. H. Zhang, et al. (PandaX Collaboration), Dark matter direct search sensitivity of the PandaX-4T experiment, *Sci. China Phys. Mech. Astron.* 43, 113001 (2019)
55. J. Liu, X. Chen, and X. Ji, Current status of direct dark matter detection experiments, *Nat. Phys.* 13(3), 212 (2017)
56. W. Zhao, et al, (CDEX Collaboration), Progress in the China Dark Matter Experiment (CDEX), *Chin. Sci. Bull.* 60(25), 2376 (2015)
57. W. Zhao, et al. (CDEX Collaboration), First results on low-mass WIMPs from the CDEX-1 experiment at the China Jinping underground laboratory, *Phys. Rev. D* 88(5), 052004 (2013)

58. H. B. Li, et al. (TEXONO Collaboration), Limits on spin-independent couplings of WIMP dark matter with a P type point-contact Germanium Detector, *Phys. Rev. Lett.* 110, 261301 (2013)
59. Q. Yue, et al. (CDEX Collaboration), Limits on light weakly interacting massive particles from the CDEX-1 experiment with a p-type point-contact germanium detector at the China Jinping underground laboratory, *Phys. Rev. D* 90(9), 091701 (2014)
60. L. T. Yang, et al. (CDEX Collaboration), Limits on light WIMPs with a 1 kg-scale Germanium detector at 160 eVee physics threshold at the China Jinping underground laboratory, *Chin. Phys. C* 42(2), 023002 (2018)
61. W. Zhao, et al. (CDEX Collaboration), Search of lowmass WIMPs with a P-type point contact Germanium detector in the CDEX-1 experiment, *Phys. Rev. D* 93, 092003 (2016)
62. C. E. Aalseth, et al. (CoGeNT Collaboration), Search for an annual modulation in three years of CoGeNT dark matter detector data, arXiv: 1401.3295 (2014)
63. L. T. Yang, et al. (CDEX Collaboration), Search for light weakly-interacting-massive-particle dark matter by annual modulation analysis with a point-contact germanium detector at the China Jinping underground laboratory, *Phys. Rev. Lett.* 123(22), 221301 (2019)
64. M. Kobayashi, et al. (XMASS Collaboration), Search for sub-GeV dark matter by annual modulation using XMASS-I detector, *Phys. Lett. B* 795, 308 (2019)
65. M. Ibe, W. Nakano, Y. Shoji, and K. Suzuki, Migdal effect in dark matter direct detection experiments, *J. High Energy Phys.* 2018(3), 194 (2018)
66. R. Agnese, et al. (SuperCDMS Collaboration), Low-mass dark matter search with CDMSlite, *Phys. Rev. D* 97(2), 022002 (2018)
67. H. Jiang, et al. (CDEX Collaboration), Limits on light weakly interacting massive particles from the first 102.8 kg × day data of the CDEX-10 experiment, *Phys. Rev. Lett.* 120(24), 241301 (2018)
68. E. Armengaud, et al. (EDELWEISS Collaboration), Searching for low-mass dark matter particles with a massive Ge bolometer operated above ground, *Phys. Rev. D* 99(8), 082003 (2019)
69. Z. Z. Liu, et al. (CDEX Collaboration), Constraints on spin-independent nucleus scattering with sub-GeV weakly interacting massive particle dark matter from the CDEX-1B experiment at the China Jinping underground laboratory, *Phys. Rev. Lett.* 123(16), 161301 (2019)
70. S. K. Liu, et al. (CDEX Collaboration), Constraints on axion couplings from the CDEX-1 experiment at the China Jinping underground laboratory, *Phys. Rev. D* 95(5), 052006 (2017)
71. Y. Wang, et al. (CDEX Collabration), Improved limits on solar axions and bosonic dark matter from the CDEX-1B experiment using the profile likelihood ratio method, *Phys. Rev. D* 101(5), 052003 (2020)
72. W. Li, et al. (CDEX Collaboration), The first result on 76Ge neutrinoless double beta decay from CDEX-1 experiment, *Sci. China Phys. Mech. Astron.* 60, 071011 (2017)
73. Z. She, et al. (CDEX Collaboration), Direct detection constraints on dark photon with CDEX-10 experiment at CJPL, arXiv: 1910.13234 (accepted by *Phys. Rev. Lett.* on Feb. 26, 2020)
74. O. Adriani, et al. (PAMELA Collaboration), The cosmicray electron flux measured by the PAMELA experiment between 1 and 625 GeV, *Phys. Rev. Lett.* 106, 201101 (2011)
75. S. Abdollahi, et al. (Fermi-LAT Collaboration), Cosmicray electron-positron spectrum from 7 GeV to 2 TeV with the Fermi large area telescope, *Phys. Rev. D* 95, 082007 (2017)
76. M. Aguilar, et al. (AMS Collaboration), Precision measurement of the $(e^+ + e^-)$ flux in primary cosmic rays from 0.5 GeV to 1 TeV with the alpha magnetic spectrometer on the international space station, *Phys. Rev. Lett.* 113, 221102 (2014)
77. O. Adriani, et al. (CALET Collaboration), Energy spectrum of cosmic-ray electron and positron from 10 GeV to 3 TeV observed with the calorimetric electron telescope on the international space station, *Phys. Rev. Lett.* 119(18), 181101 (2017)
78. E. S. Seo, et al. (CREAM Collaboration), Cosmic ray energetics and mass for the international space station (ISS-CREAM), *Adv. Space Res.* 53(10), 1451 (2014)
79. O. A. Driani, et al. (PAMELA Collaboration), An anomalous positron abundance in cosmic rays with energies 1.5–100 GeV, *Nature* 458, 07942 (2009)
80. J. Chang, et al. (DAMPE Collaboration), The dark matter particle explorer mission, *Astropart. Phys.* 95, 6 (2017)
81. G. Ambrosi, et al. (DAMPE Collaboration), Direct detection of a break in the teraelectronvolt cosmic-ray spectrum of electrons and positrons, *Nature* 552(7683), 63 (2017)
82. Y. Z. Fan, W. C. Huang, M. Spinrath, Y. L. S. Tsai, and Q. Yuan, A model explaining neutrino masses and the DAMPE cosmic ray electron excess, *Phys. Lett. B* 781, 83 (2018)
83. P. H. Gu and X. G. He, Electrophilic dark matter with dark photon: From DAMPE to direct detection, *Phys. Lett. B* 778, 292 (2018)
84. P. Athron, C. Balazs, A. Fowlie, and Y. Zhang, Model-independent analysis of the DAMPE excess, *J. High Energy Phys.* 2018(2), 121 (2018)
85. T. Li, N. Okada, and Q. Shafi, Scalar dark matter, type II seesaw and the DAMPE cosmic ray e^+e^-excess, *Phys. Lett. B* 779, 130 (2018)
86. G. Liu, F. Wang, W. Wang, and J. M. Yang, Explaining DAMPe results by dark matter with hierarchical lepton-specific Yukawa interactions, *Chin. Phys. C* 42(3), 035101 (2018)
87. S. Ge, H. J. He, and Y. C. Wang, Flavor structure of the cosmic-ray electron/positron excesses at DAMPE, *Phys. Lett. B* 781, 88 (2018)